

Original Research Article

Isoconversional and Model-fitting approaches to Kinetic and Thermoanalytic study of Lanthanum oxalate: Nonlinear relationship between kinetic parameters.

ABSTRACT

The data for the nonisothermal and isothermal thermal decompositions of lanthanum oxalate have been analysed using the model-free and model-fitting kinetic techniques. When applied to nonisothermal data using the Coats-Redfern (CR) equation, the widely used model-fitting approach that results excellent fitting for both isothermal and nonisothermal data but produces very ambiguous values of the Arrhenius parameters. These values cannot be compared to those obtained from isothermal experiments. On the other hand, the model-free strategy represented by the iso-conversional method, such as Flynn-Wall-Ozawa (FWO) and Kissinger-Akahira-Sunose (KAS), emphasize proportionate variation of the activation energy with the degree of conversion for both isothermal and nonisothermal experiments. The model free approach is recommended as a reliable way for obtaining consistent kinetic information from both isothermal and non-isothermal data. Despite their linear correlation, the kinetic parameters do not exhibit isokinetic behaviour. Thus, utilising Nonlinear Compensation Law, a greater association between kinetic triplets was examined.

Keywords: Nonisothermal decomposition, Model free and model fitting methods, Kinetic parameters, Thermodynamic parameters, Isokinetic behaviour, Nonlinear compensation law

1. INTRODUCTION:

For many researchers, kinetic study of thermal breakdown processes has been a particularly interesting topic. The breakdown processes and kinetics go hand in hand. Understanding the mechanism enables the postulation of kinetic equations, or the other way around [1]. It is obvious that choosing the right model is a crucial step in kinetic analysis. Several scholars have assessed how a model may support experimental data [2–3]. The kinetics of non-isothermal processes can be investigated using a variety of techniques. They include iso-conversional model-free techniques, statistical techniques, and the Coats-Redfern (CR) method. For the defined conversion intervals, activation energy, or E_a values, were obtained [4] by utilising the iso-conversional model-free procedures such as modified Kissinger-Akahira-Sunose (KAS) and the Kissinger method, respectively. E and the change in entropy ΔS^* for the creation of the activated complex from the

reagents have also been shown to be linearly related. These dependencies are connected to the presumption that the composites under study experienced the same kinetic mechanisms of heat deterioration [5].

The Coat-Redfern (CR) method exhibits nonlinear trends for reactions with heterogeneous mechanisms, and the reaction models and kinetic parameters cannot be retrieved from the curves. As a result, the method is often inappropriate for determining kinetic parameters[6]. The average findings of non-isothermal trials may be compared with isothermal analysis since using the standard methods in non-isothermal kinetics leads in highly ambiguous Arrhenius parameter values that cannot be properly compared with isothermal values [7]. The iso-conversional method serves as the foundation for an alternative model-free methodology. The application of this model-free method in both isothermal and non-isothermal kinetics helps in avoiding issues that result from the inappropriate evaluation of reaction model. The model-free methodology allows the proportionate variation of activation energy with the degree of conversion. As a result, it is possible to estimate reaction rates with accuracy and make mechanistic conclusions [8]. The exact activation energy cannot therefore be inferred from a single non-isothermal curve. On the other hand, the correct kinetic parameters can be identified clearly when a collection of curves is recorded using various heating regimens [9]. According to experimental findings, the values of the kinetic parameters obtained using the model-free and model-fit approaches are in close agreement and can be utilised to comprehend the decomposition mechanism of solid-state reactions [10].

The present work apply both model-fitting integral and model-free isoconversional methods to have significant and appreciable picture about the decomposition mechanism of Lanthanum Oxalate Decahydrate. The degree of reliability of parameters obtained from both the techniques are also studied. The kinetic parameters which generally fit to linear kinetic compensation law[11] have been revisited for better correlation from their nonlinearity and the authenticity of the kinetic data was tested by fitting into nonlinear compensation law so as to obtain true values.

2. MATERIAL AND METHODS:

Lanthanum Oxalate Decahydrate, was prepared as per our earlier work[12], using high purity AR grade $\text{La}(\text{NO}_3)_3$ and Ammonium Oxalate purchased from Sigma –Aldrich. Ammonium Oxalate solution was added drop wise to the $\text{La}(\text{NO}_3)_3$ solution with stirring for 30 min. White precipitate of Lanthanum Oxalate decahydrate (LaOx) obtained was washed with distilled water and absolute alcohol. For one hour, the precipitate was allowed to stand at room temperature. Powdered lanthanum oxalate decahydrate was produced after being ground in an agate mortar and dried in a vacuum oven at 70°C . By using FTIR, TEM, XRD, etc., the obtained Lanthanum oxalate powder was characterised. The calcination products were produced by heating for 1 hour at a range of temperatures ($200\text{--}800^\circ\text{C}$) in a static air atmosphere. The results of the thermal analysis were used to determine the calcination temperatures. LaOx-200 designates the calcination product at 200°C , and the calcination products are indicated throughout the article by the oxalate designation and the temperature used. Thermal TG/ DTA analysis of lanthanum oxalate were carried out at the heating rates of $3, 5$ and 7°C min^{-1} up to 900°C in a dynamic atmosphere of air (20 ml/min), using **SHEMATZU DTG 50 analyzer**. The same sample was also subjected to isothermal breakdown at temperatures of $643, 653,$ and 663K .

3. RESULTS AND DISCUSSIONS:

3.1. FTIR analysis

The FT-IR 410 JASCO(JAPAN) on KBr support was used to obtain the IR spectra across the wavelength range of $4000\text{--}100\text{ cm}^{-1}$. $\text{La}_2(\text{C}_2\text{O}_4)_3 \cdot 10\text{H}_2\text{O}$ and the Lanthanum oxalate calcined at 200°C (Fig. 1) are quite similar in structure, with the oxalate anions' ($1750\text{--}640\text{ cm}^{-1}$) and the water of hydration ($3440, 1640\text{ cm}^{-1}$) absorption bands being the most similar. IR-spectrum of Lanthanum oxalate calcined at 300°C , the $\text{C}_2\text{O}_4^{2-}$ species are weaker than CO_3^{2-} and exhibit distinctive CO_3^{2-} like bands at 2350 cm^{-1} and $1800\text{--}400\text{ cm}^{-1}$. Further heating at 400°C causes lose water of bands due to hydration absorption. The fundamental modes of vibration of the CO_3^{2-} species are weakened and distinct band structure appear at $1600\text{--}1300\text{ cm}^{-1}$ corresponding to characteristic absorptions of oxycarbonates. The IR-spectrum LaOx-550 exhibits substantial oxycarbonate with additional bands at $1060\text{--}870\text{ cm}^{-1}$. The La-O vibrational bands appear at $730\text{--}500\text{ cm}^{-1}$. The IR-spectrum of lanthanum Oxalate calcined at 800°C , shows no absorptions due to oxycarbonate species. Lattice vibration modes of La_2O_3 are related to the absorptions below 700 cm^{-1} . Given that La_2O_3 is a recognised basic

oxide, the weak bands at 1600, 1500, and 1380 cm^{-1} are most likely caused by carbonate and moisture on the surface.

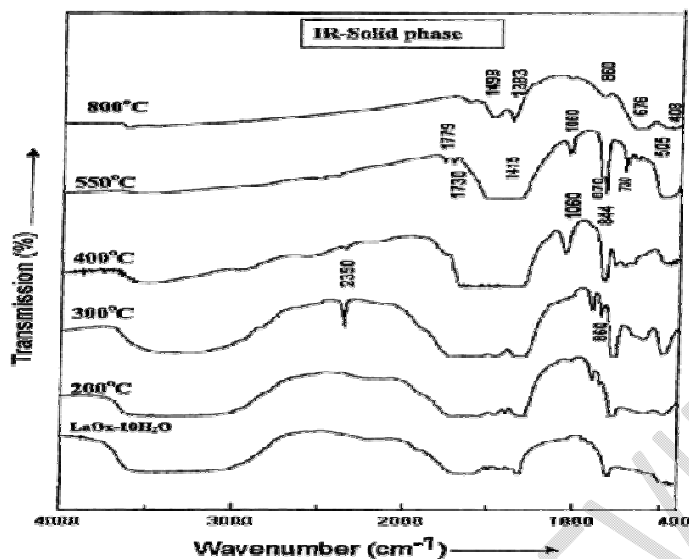


Fig.1: FTIR curves of Lanthanum Oxalate at room temperature at temperatures 200, 300,400,550 & 800°C

3.2. TEM Analysis :

The general morphologies and microstructure of the sample was investigated by transmission electron microscopy (TEM, JEM-100CX II, Japan Electronics Co., Ltd., Japan), which illustrates that many needle-shaped particles are in the size range of 100 nm. The TEM images (Fig.2) reveal that most of the particles are uniform in size.

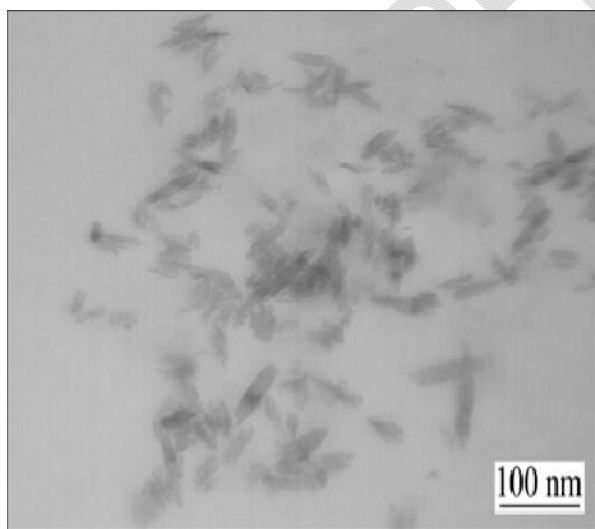


Fig.2: TEM image of lanthanum Oxalate decahydrate

3.3. Thermal Analysis with X-ray diffraction:

Using a rising temperature approach at 10 min^{-1} till 900°C in air, the non-isothermal decomposition of the uniform 300 mesh lanthanum oxalate decahydrate $\text{La}_2(\text{C}_2\text{O}_4)_3 \cdot 10\text{H}_2\text{O}$ is examined (Fig. 4). Shimadzu XRD-6000 diffractometer X-ray diffraction patterns were obtained by scanning the angular range $100 \leq 2\theta \leq 900$ using $\text{CuK}\alpha$ radiation ($\lambda = 1.5418 \text{ \AA}$). Intermediates and

final solid products were characterised by FTIR-spectroscopy and X-ray diffraction (XRD). The results show that $\text{La}_2(\text{C}_2\text{O}_4)_3 \cdot 10\text{H}_2\text{O}$ dehydrates in stepwise at 90–360°C. The intermediates, $\text{La}_2(\text{C}_2\text{O}_4)_3$, $\text{La}_2\text{O}(\text{CO}_3)_2$ and $\text{La}_2\text{O}_2\text{CO}_3$, were formed at 400, 425 and 470°C, respectively. The final product La_2O_3 obtained at 800°C [13].

The XRD patterns (Fig. 3) of LaOx-200 and LaOx-400 indicates that the products are amorphous indicating $\text{La}_2(\text{CO}_3)_3$ product to be amorphous.

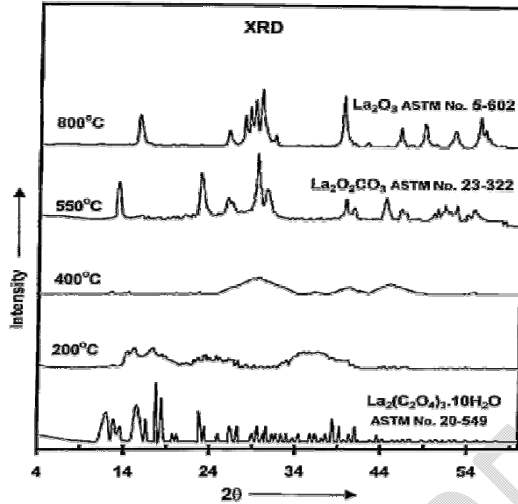


Fig. 3 : X-Ray diffraction patterns of decomposition products of lanthanum oxalate obtained at different temperatures

The conversion of $\text{La}_2(\text{CO}_3)_3$ to $\text{La}_2\text{O}(\text{CO}_3)_2$ which converts immediately to $\text{La}_2\text{O}_2\text{CO}_3$ as follows [12]:

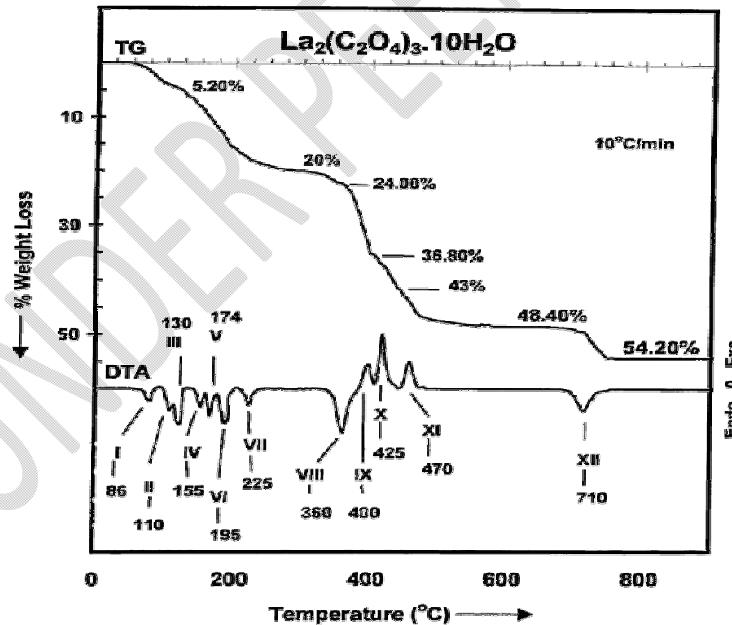
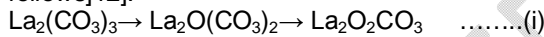
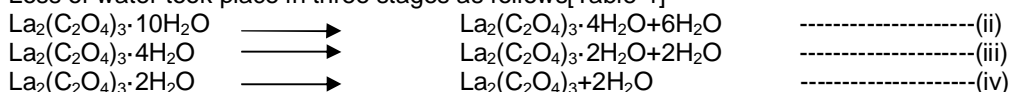


Fig.4: TG-DTA curve of Decomposition of Lanthanum Oxalate decahydrate heated up to 900°C

Events IX, X, and XI took place between 420–550°C. The aforesaid reaction is supported by the IR spectra (Fig.1) and XRD patterns (Fig.3). The comparable X-ray pattern for LaOx-550 displays the crystalline $\text{La}_2\text{O}_2\text{CO}_3$ pattern. X-ray pattern of LaOx-800 reveals a crystalline phase of La_2O_3 in support of FTIR.

Loss of water took place in three stages as follows[Table-1]



The fourth stage begins at 375 °C involving decomposition of $\text{La}_2(\text{C}_2\text{O}_4)_3$ to $\text{La}_2\text{O}_2(\text{CO}_3)$, a dioxy monocarbonate[12].

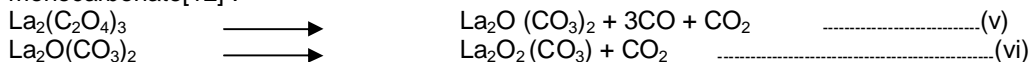
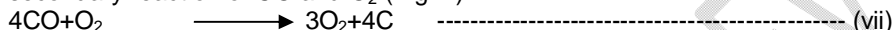


Table 1: Step wise Degradation data of $\text{La}_2(\text{C}_2\text{O}_4)_3 \cdot 10\text{H}_2\text{O}$

Temperature Range/ ^o C	Mass change (%)		Solid residue
	Theoretical	Experimental	
30–225	14.7	14.5	Hexahydrate
225–300	5.2	4.98	Dihydrate
300–375	4.98	5.12	Anhydrous oxalate
375–600	23.7	28.52	$\text{La}_2\text{O}_2\text{CO}_3$
600–750	6.19	6.92	La_2O_3

Although the decomposition of oxalate is endothermic, the exotherms appear in DTA is due to secondary reaction of CO and O₂ (Fig. 4).



3.4. Kinetic Analysis :

For determination of Kinetic parameters, the TG curves are obtained at heating rates of 3, 5, and 7°C min⁻¹ (Fig.5), show that the sample degraded between 370 °C and 550 °C. The maximum decomposition temperature, T_m and inception temperature T₀ increase with rate of heating. Furthermore, the area under the decomposition peak increased with increasing heating rate (Fig. 6).

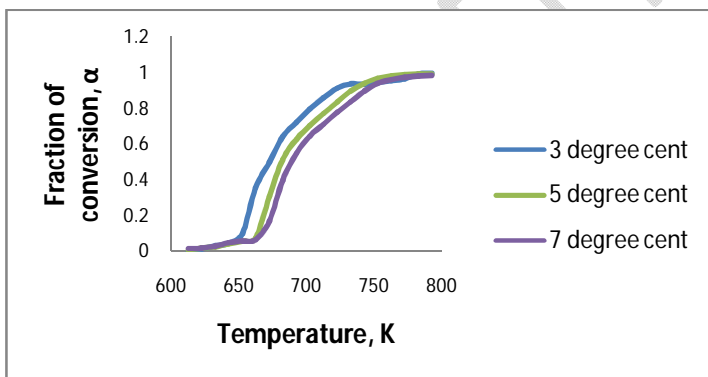


Fig.5 : Thermogravimetric curves for decomposition of lanthanum oxalate at different rate of heating

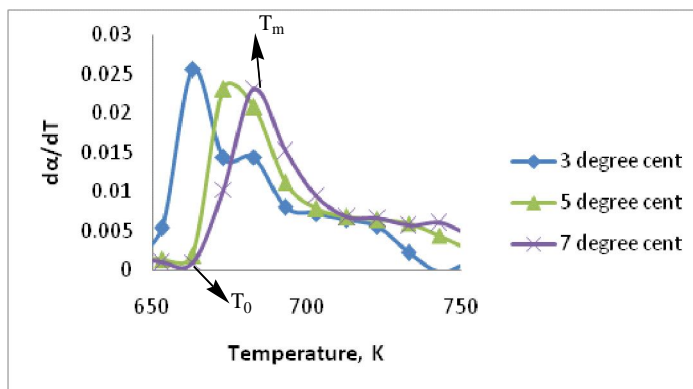


Fig.6: Derivative curves of lanthanum oxalate decomposition at different rates of heating

Isothermal decomposition curves for the lanthanum oxalate at three different temperatures also exhibit similar behaviour as in case of non-isothermal study and the “conversion-time” curve i.e. ‘ α -t’, plot show upward shift with time, at higher temperatures (Fig.7).

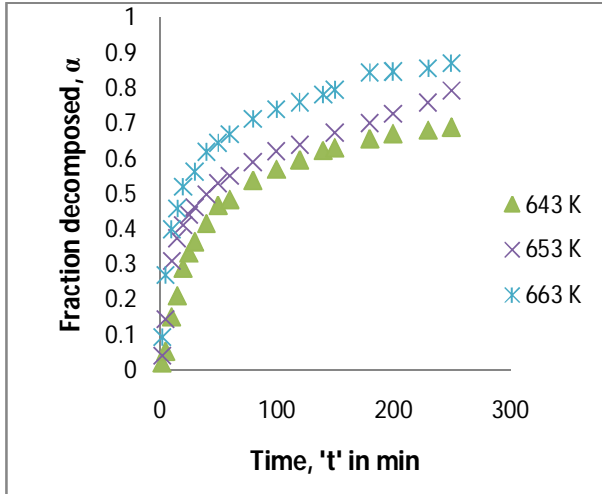


Fig.7: Conversion- time curve for isothermal decomposition of lanthanum oxalate

3.4.1. Nonisothermal method:

Model-fitting Coat Redfern (CR) and iso-conversional model free (FWO & KAS) approaches were both used to determine kinetic parameters[15]. At the temperature range of 380-480°C, or 653-753K (steps VIII-XI), for the best-fitting F3 mechanism model functions, $g(\alpha)$, and correlated by the compensation law[16], the Arrhenius parameters E and $\log A$ are derived. Using the CR equation, the slopes and intercepts of the graphs $1/T$ vs. $\log [g(\alpha)/T^2]$ at three different heating rates are obtained (Fig. 8):

$$\log [g(\alpha)/T^2] = \log [AR/\beta E] - E/2.303RT \dots\dots\dots(3).$$

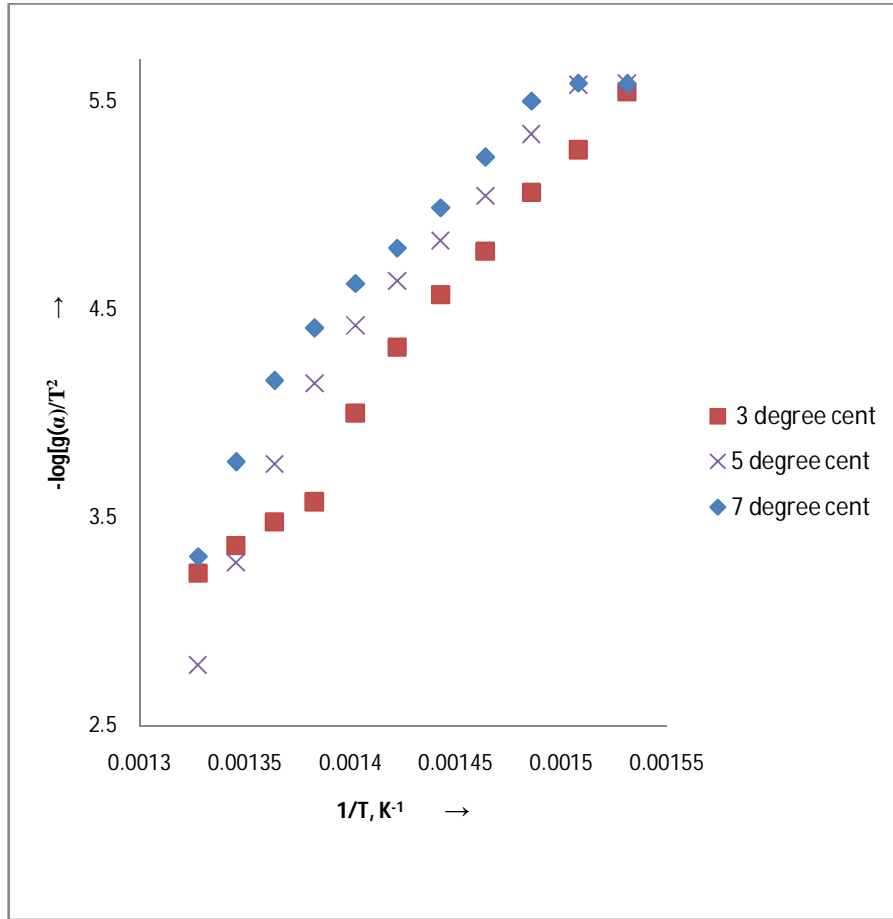


Fig.8: Variation of $-\log[g(\alpha)/T^2]$ with $1/T$ at different rate of heating

Iso-conversional analyses allow a complex processes to be detected by variation of E_α with α . The Kissinger–Akahira–Sunose(KAS) method is used in the form

$$\ln(\beta/T_\alpha^2) = \ln(A_\alpha R)/(E_{a,\alpha}g(\alpha) - E_{a,\alpha}/R T_\alpha) \dots\dots\dots(4)$$

Thus, for different values of α , $\ln(\beta/T_\alpha^2)$ and $1/T_\alpha$, were obtained from thermal curves at different heating rates, and straight lines are obtained for each ' α ' (Fig.9).The apparent activation energies, E and pre-exponential factors, logA are evaluated from the slopes and intercepts respectively.

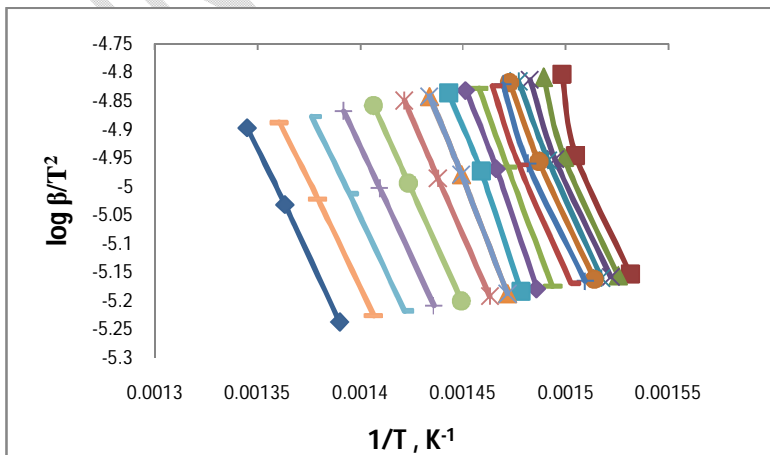


Fig 9: $\ln(\beta/T_a^2)$ vs $1/T_a$ plots

Similarly the Flynn–Wall–Ozawa (FWO) method is used in the form [17]

$$\ln \beta = \ln (A_a E_{a,a} / (Rg(\alpha)) - 5.331 - 1.052 E_{a,a} / (RT_a) \text{ -----(5)}$$

A graph between $\ln \beta$ and $1/T_a$, are plotted for different α 's (Fig.10) which allow us to evaluate the E and $\log A$. The average values are calculated for comparison (Table-3).

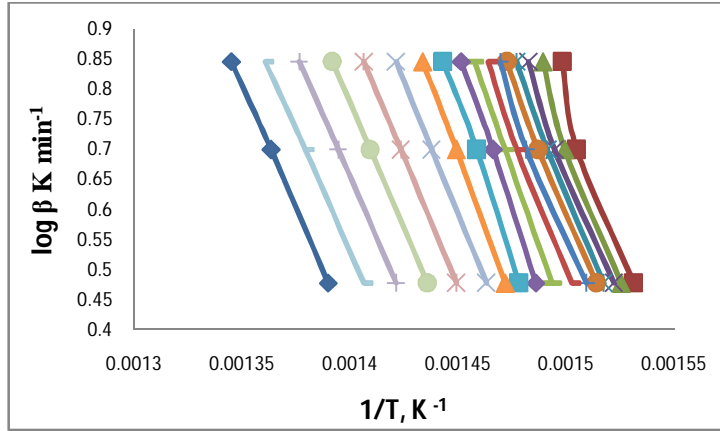


Fig.10 : $\log\beta$ — $1/T$ plots for E of the first endothermic peak by FWO method

3.4.2. Isothermal method:

Isothermal study in the temperature region 643-663K allow the calculation of kinetic parameters by correlating mechanism model function, $g(\alpha)$ with time ,t(Fig.11).The plot is a straight line with rate constant, k calculated from the slope using the equation:
 $g(\alpha)= kt + c$(1)

The rate, k was obtained at three different isothermal temperatures and presented [Table 3].The kinetic parameters E and A are obtained from slope and intercepts respectively, from the plot of $\ln k$ vs $1/T$ (Fig.12) using the Arrhenius equation ;
 $\ln k = \ln A - E/RT$ (2)

The isothermal and non-isothermal kinetic parameters are compared and presented in Table 2.

Table 2: Kinetic and Thermodynamic parameters of $La_2(C_2O_4)_3$ decomposition, by various methods

	$\beta, (^{\circ}Cmin^{-1})$	E,(kJmol ⁻¹)	log A,(min ⁻¹)	$\Delta H^*,(kJmol^{-1})$	$\Delta S^*(Jmol^{-1}K^{-1})$	$\Delta G^*(kJmol^{-1})$
Coat-Redfern Method	3	230.33	16.00	224.76	46.34	193.71
	5	255.50	17.94	249.92	83.46	194.01
	7	209.26	14.32	203.69	14.26	194.13
	Average	231.70	16.09	226.12	48.02	193.95
Isoconversional Methods	FWO	167.98	11.05	162.41	-48.46	194.88
	KAS	165.26	10.06	159.69	-52.25	194.70
Isothermal Method		303.03	23.16	298.77	148.19	199.48

Table 3 :Rate constants obtained at different isothermal temperatures

k ,sec ⁻¹	T,K	1/T, K ⁻¹	-log k
0.038819	643	0.00155521	1.41096
0.069832	653	0.001531394	1.15595
0.215161	663	0.001508296	0.66724

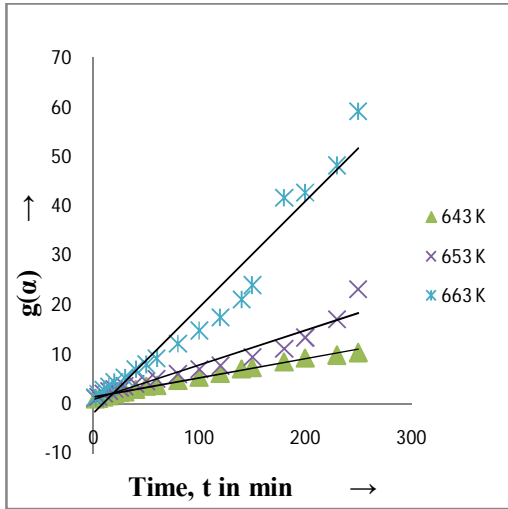


Fig.11: Variation of $g(\alpha)$ with time ,t at different temperatures

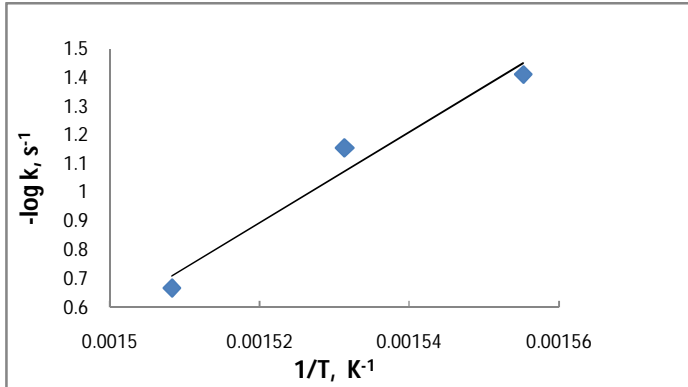


Fig.12 : Variation of T^{-1} with $-\log k$ during isothermal decomposition of lanthanum oxalate

The apparent activation energy for the degradation of lanthanum Oxalate is not same at all conversion, α (Fig. 13), indicates the existence of a complex multistep mechanism that occurs in the solid state. The kinetic and thermodynamic parameters for both model fitting and model free methods are presented [Table 2].

The values of apparent activation energy (E_a) calculated by model free (KAS and FWO) methods are in conformity with the reported activation energy in many studies i.e. 177.5 kJ/mol [18] and lower than values of E_a calculated by integral non- isothermal (Coat-Redfern) and isothermal methods . Thermodynamic parameters e.g. entropy of activation (ΔS^*), enthalpy of activation (ΔH^*) and Gibbs free energy (ΔG^*) were calculated using Equations (6)-(9).

$$A = (kT/h)e^{(\Delta S^*/R)} \quad \dots\dots\dots (6)$$

$$\Delta H^* = \Delta E - RT \quad \dots\dots\dots (7)$$

$$\Delta G^* = \Delta H^* - T\Delta S^* \quad \dots\dots\dots (8)$$

where h and k are Planck's constant and Boltzmann constant respectively.

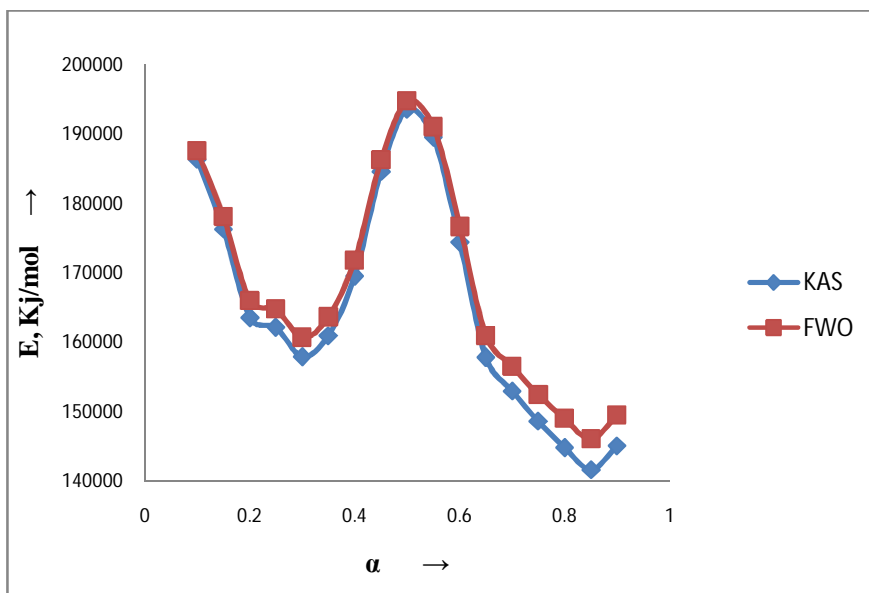


Fig. 13: Variation of activation energies, E with degree of conversion, α

With an increase in activation energy, it has been found that the entropy of activation also increases. The fact that the value of ΔG is positive indicates that the Lanthanum oxalate decomposition process is not spontaneous. It is noted that the activation energy is nearly equal to the activation enthalpy, which suggests that lanthanum oxalate is in the condensed phase between 653 and 753 K. When ΔS^* values for iso-conversional procedures are negative, it means that the activated complex for that method has a higher degree of arrangement (lower entropy) than it had in the initial state. Table 3 presents information on kinetic and thermodynamic characteristics gathered by various techniques.

In case of isothermal method the E has the highest value and this discrepancy may be due to the F3 mechanism which could be different in case of isothermal study. Moreover the rising temperature technique that uses CR equation with F3 model function also reported higher value of E. This may be attributed to the fact that, for $\alpha < 0.70$ in the chosen temperature range and the plot of $\log[g(\alpha)/T^2]$ versus $1/T$ is linear, indicating that the reaction is a single mechanism. However for extents of reaction $\alpha > 0.7$ the reaction has multi model mechanisms, for which the CR eqn. cannot be used showing a nonlinear trend (Fig.8). Therefore it is ascertained that kinetics of complex reactions, where the reaction model changes with the extent of reaction, cannot be analysed with CR method with absolute correctness.

Further from isoconversional methods it is evident that E depends on α , demonstrating that the decomposition reaction process of the lanthanum oxalate is of complex kinetic mechanism [19]. Hence the kinetic parameters derived may be considered to be apparent and not true. The activation energies, E calculated by various methods are presented in bar diagram(Fig. 14)

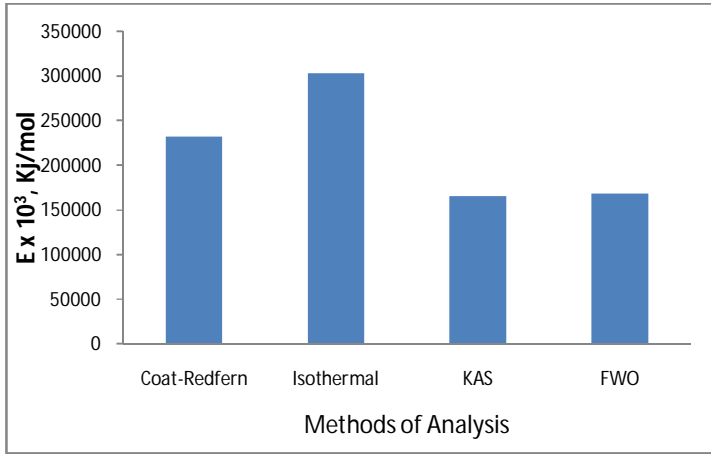


Fig. 14: variation of activation energies with methods of analysis

3.4.3. Kinetic compensation effect:

The change in apparent activation energy, E , is found to be followed by a change in $\ln A$. This phenomenon is known as the kinetic compensation effect (KCE), and it frequently coexists with the isokinetic point ($1/T_{iso}$, $\ln k_{iso}$). According to the Cremer-Constable relation, the variations in pre-factor and apparent activation enthalpy exhibit a linear dependency[20].

$$\ln A = aE + b \quad \dots\dots\dots(9)$$

Where a and b are constant coefficients for a series of related rate process and are called compensation parameters. The rate constant, ' k ' is temperature dependent, and is usually described well by Arrhenius relationship:

$$k = A e^{-E_a/RT} \quad \dots\dots\dots(10)$$

$$\ln A = \ln k + E/RT \quad \dots\dots\dots(11)$$

Although the experimental data showed that a plot of $\ln A$ vs E (Fig.16) and $\log k$ vs $1/T$ (Fig.15) different methods in the temperature range 653K-753K, are all linear, but fail to display a single point of concurrence i.e. isokinetic point ($1/T_{iso}$, $\log k_{iso}$). Hence the kinetic parameters exhibit a false compensation effect and are with their apparent values.

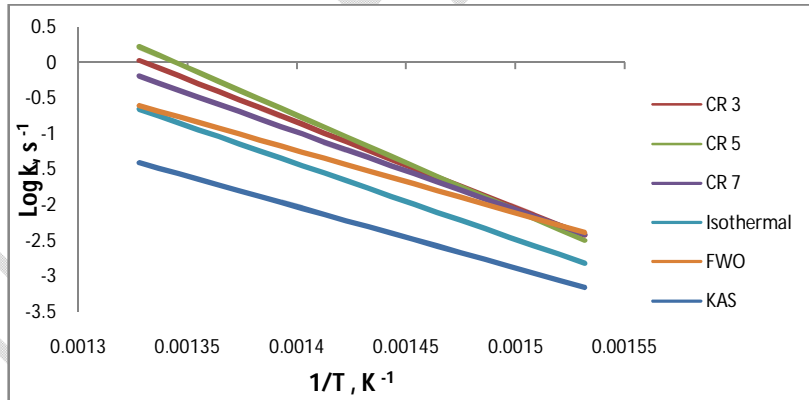


Fig.15 : Variation of log k with 1/T for different methods of analyses.

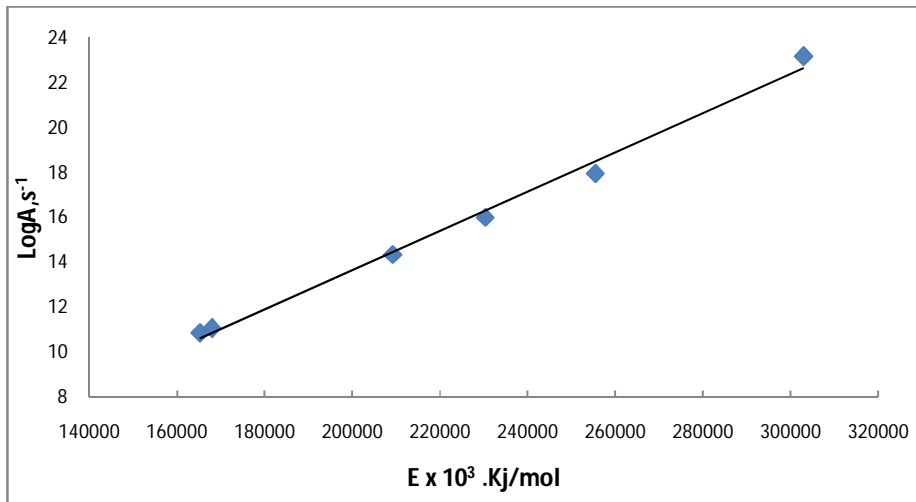


Fig.16: Variation of log A with E and verification of Kinetic Compensation Effect

3.4.4. Non linear Compensation law and kinetic parameters:

The correlation derived between the kinetic parameter E and logA' from TG curves can be described by means of Non linear compensation law[21] expressed as $\log A' = (RT_{0.1} \ln 10)^{-1} E + \log(\beta E / T_{0.1}^2) - 1.85$ (12)

Where $T_{0.1}$ is the temperature at which the conversion attains a degree of 0.1 ($\alpha = 0.1$). The equation is not a linear and therefore it is not an iso-kinetic relation. However the relationship becomes iso-kinetic provided $\log(\beta E / T_{0.1}^2)$ is constant, which is not found in the present work. The true values of pre factor logA' is varies with rates of heating, β and presented along with $\log(\beta E / T_{0.1}^2)$ [Table-4] for both model fitting and model free methods of analyses.

Table-4: Corrected approximation for pre-exponential factors using nonlinear compensation law

	β	$\log(\beta E / T_{0.1}^2)$	$\log A', (s^{-1})$
CR	3	0.2096	16.572
	5	0.4614	18.692
	7	0.5169	15.04
FWO	3	0.0725	11.657
	5	0.2792	11.632
	7	0.4214	11.715
KAS	3	0.0655	11.433
	5	0.2721	11.411
	7	0.4144	11.495

4. CONCLUSION

It was ascertained that using model-fitting techniques of kinetic analysis to data obtained under non-isothermal experimental settings does not allow for the accurate determination of the activation energy. As the ICTAC Kinetics Committee has advised [22], it is therefore required to employ a set of curves obtained under various heating regimens. As only one-step processes may be analysed using this methodology, it is also important to consider the nature of the reaction under study into account.. Isoconversational techniques or the deconvolution of the separate steps, such as KAS and FWO, are

required for more complicated or multi-step reactions. The kinetic parameters of the conversion of lanthanum oxalate to the equivalent carbonate follow kinetic compensation behaviour, but the result is an false compensation effect. Non-linear compensation rule, which is a good approximation, provides a more accurate explanation of the relationship between E and logA.

COMPETING INTERESTS

There is not any potential conflicts of interest like employment, consultancies, honoraria, paid expert testimony, patent applications/registrations, and grants or other funding etc. There is no financial and personal relationships with other people or organizations that could inappropriately influence (bias) the work.

REFERENCES

- [1] J. Jach in "reactivity of solids" (Ed. J.H. De. Boer) Elsevier, Amsterdam, 1961 pp. 334
- [2] J.Jach; The thermal decomposition of NaBrO_3 part I-Unirradiated material, J. Phys, Chem solids 1963, 24, 63
- [3] A.K.Galway,in "Int.Rev.Sc."Inorg.chem.Series II.Butterworth, London 1975, 10,147
- [4] V.V.Boldyrev, Topochemistry of Thermal decomposition of solids, Thermochim.Acta,1986 100, 315
- [5] J.Physiak, and B.P.Wasia J.Therm.Anal,1984,29, 829
- [6] R.Ebrahimi-Kahrizsangi,M.H. Abbasi; Evaluation of reliability of Coats-Redfern method for Kinetic analysis of non-isothermal TGA. Trans. Nonferrous Met. Soc. China,2008, 18,217-221
- [7] Xia Yongjiang, XueHuaqing, Wang Hongyan, Li Zhiping, Fang Chaohe; Kinetics of isothermal and non-isothermal pyrolysis of oil shale; Oil Shale, 2011, 28, 415-424
- [8] Sergey Vyazovkin and Charles A. Wight; Isothermal and non-isothermal kinetics of thermally stimulated reactions of solids; Int. Rev. in Phy. Chem. , 1998, 17, 407- 433
- [9] Pedro E Sánchez-Jiménez, Luis A Pérez-Maqueda, Antonio Perejón and José M Criado Clarifications regarding the use of model-fitting methods of kinetic analysis for determining the activation energy from a single non-isothermal curve; Chem. Cent. Journal 2013, 7,25(Short Communication)
- [10] K. Slopiecka, P. Bartocci, F. Fantozzi; Thermogravimetric analysis and Kinetic study of poplar wood pyrolysis Third International Conference on Applied Energy 2011: 1687-1698
- [11] Z.Adonyi and G.Korosi; Experimental Study of Non-isothermal Kinetic equations and compensation effect; Thermochim. Acta, 1983, 60: 23-45
- [12] Nayak H, Pati S . K, Bhatta. D. Decomposition of γ -irradiated $\text{La}_2(\text{C}_2\text{O}_4)_3 + \text{CuO}$ mixture: A non-isothermal study ; Rad. Eff. and Def. in Solids, 2004, 159: 93-106.
- [13] Basma A.A. Balboul, A.M. El-Roudi, Ebthal Samir, A.G. Othman; Non-isothermal studies of the decomposition course of lanthanum oxalate decahydrate, Thermochim. Acta,2002 387:109-114
- [14] P.Simon, Isoconversional methods-Fundamental, meaning and application; J. Therm. Anal. Calorim. 2004, 76:123
- [15] S. Vyazovkin, C.A. Wight, Model free and model fitting approaches to Kinetic analysis of isothermal and nonisothermal data; Thermochim. Acta, 1999, 340/341: 53
- [16] B.Jankovic; Kinetic analysis of the nonisothermal decomposition of potassium metabisulfite using the model-fitting and isoconversional (model-free) methods; Chem. Eng. Journal, 2008, 139:128-135
- [17] ZHAN Guang, YU Jun-xia, XU Zhi-gao, ZHOU Fang, CHIRu-an; Kinetics of thermal decomposition of lanthanum oxalate hydrate ; Trans. Nonferrous Met. Soc. China, 2012, 22: 925-934
- [18] Obaid A Y, Alyoubi A O, Samarkandy A A, Al-Thabaiti S A, Al-Juaid S S, Ei-Bellhi A A, Ei-Deifallah H M.; Kinetics of thermal decomposition of copper(II) acetate monohydrate. J. Therm Anal Calorim, 2000, 61(3): 985-994.
- [19] Bond, G. C.; Keane, M. A.; Kral, H.; Lercher, J. A. Catal. Rev.-Sci. Eng. 2000, 42(3): 319-327
- [20] J. Zsako, Kinetic analysis of Thermogravimetric data xxxi. Derivation of non-linear kinetic compensation law, J. Therm. Anal., 1998, 54:921-929

[21]Vyazovkin S, Burnham AK, Criado JM, Perez-Maqueda LA, Popescu C, Sbirrazzuoli N: ICTAC Kinetics Committee recommendations for performing kinetic computations on thermal analysis data. *Thermochim. Acta*, 2011, 520:1–19.

UNDER PEER REVIEW